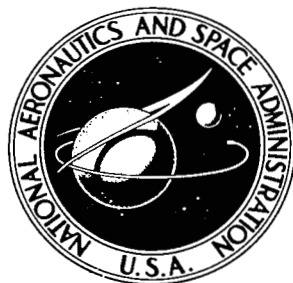


NASA TECHNICAL NOTE



NASA TN D-4639

0.1



NASA TN D-4639

LOAN COPY: RETURN TO
AFWL (WLIL-2)
KIRTLAND AFB, N MEX

SOUND MEASUREMENTS ON A FULL-SCALE JET-ENGINE INLET-NOISE-SUPPRESSOR COWLING

by L. Jack Smith, Loren W. Acker, and Charles E. Feiler

Lewis Research Center

Cleveland, Ohio



NATIONAL AERONAUTICS AND SPACE ADMINISTRATION • WASHINGTON, D. C. • JULY 1968



**SOUND MEASUREMENTS ON A FULL-SCALE JET-ENGINE
INLET-NOISE-SUPPRESSOR COWLING**

By L. Jack Smith, Loren W. Acker, and Charles E. Feiler

**Lewis Research Center
Cleveland, Ohio**

NATIONAL AERONAUTICS AND SPACE ADMINISTRATION

For sale by the Clearinghouse for Federal Scientific and Technical Information
Springfield, Virginia 22151 - CFSTI price \$3.00

ABSTRACT

Several prototype suppressors were ground tested on a jet engine. Broadband resonant absorbers were used as the acoustic absorption treatment. Inlet geometries included both acoustically treated struts and a circumferential splitter ring. Results of calculations on far-field noise data showed a maximum total sound power reduction of 10.2 decibels and simulated flyover noise reductions up to 10.5 perceived noise decibels. Strut geometries were best for sideline noise reduction, but the splitter configuration, with the most treated surface area, achieved the greatest sound power reduction. A mathematical model of sound power attenuation correlated with the data.

STAR Category 02



SOUND MEASUREMENTS ON A FULL-SCALE JET-ENGINE INLET-NOISE-SUPPRESSOR COWLING

by L. Jack Smith, Loren W. Acker, and Charles E. Feiler

Lewis Research Center

SUMMARY

Several prototype full-scale inlet noise suppressors were ground tested on a jet engine. The suppressors used broadband resonant absorbers as the acoustic absorption treatment. Inlet geometries included both acoustically treated struts and a circumferential splitter ring. The results of calculations on the far-field noise data showed a maximum total sound power reduction of 10.2 decibels and simulated flyover noise reductions up to 10.5 perceived noise decibels. Strut geometries proved best at sideline noise reduction, but the splitter configuration, which had the most treated surface area, achieved the greatest sound power reduction. A mathematical model of sound power attenuation as a function of the physical properties of the acoustical treatment correlated with the data.

INTRODUCTION

Compressor and fan noise on commercial jet aircraft engines can be reduced by engine redesign or by installation of inlet and fan exhaust noise suppressors. This report presents the results of an experimental program on an inlet noise suppressor having a broadband resonant absorber. The design of several full-scale inlet noise suppressors and the far-field noise reduction obtained with their installation on a modified Curtiss-Wright J-65 engine are given.

A considerable amount of work has been done on identifying compressor and fan noise sources and in developing noise reduction techniques. Reference 1 summarizes most of the general noise reduction techniques associated with fan and compressor noise. Reference 2 gives more detailed design requirements for inlet and fan exhaust noise suppressors, and, in particular, presents some data for suppressor design using absorptive materials. These data were obtained from model and full-scale inlet sections

that were lined with absorptive materials to obtain a resonant-type noise suppressor. The liner surface is a layer of porous material made of bonded metallic fibers. The porous layer is separated from an impervious back wall by an air gap that causes the liner to behave like a Helmholtz resonator with broadband absorption ability. With the use of various porous materials and varying thicknesses of the air-gap backing, the resonator can be tuned to absorb noise across the fan-compressor noise region of the spectrum. Far-field noise data on full-scale inlet noise suppressors of this type are lacking; thus, the expected sound power and flyover noise reduction are experimentally undetermined.

The objectives of the program at the NASA Lewis Research Center were to design and construct a full-scale inlet noise suppressor with a broadband resonator-type liner and to obtain far-field noise measurements when the suppressor was mounted on a jet engine. Several suppressors were designed that would change the amount of treated surface area and the inlet configuration. Measurements on an untreated reference inlet cowling were made and used as a basis for determining the noise reduction of the treated inlets.

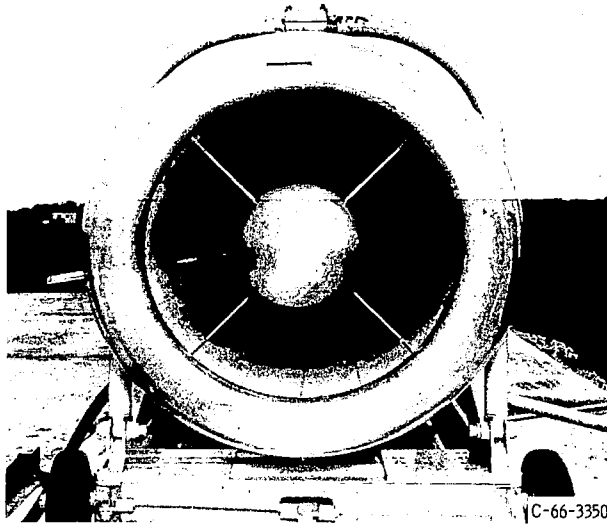
Primary design goals concerned acoustic fan noise reduction; no effort was made to produce hardware appropriate for flight use. Simplified inlet geometries were used for ease of construction, and it was expected that some thrust losses would be incurred.

Described herein are the suppressor design, the techniques used to convert the J-65 turbojet engine to a sound source having the properties of a turbofan, and the results of far-field measurements of sound attenuation and aerodynamic performance losses. A mathematical model that correlates sound power attenuation with physical properties of the acoustic treatment is also described.

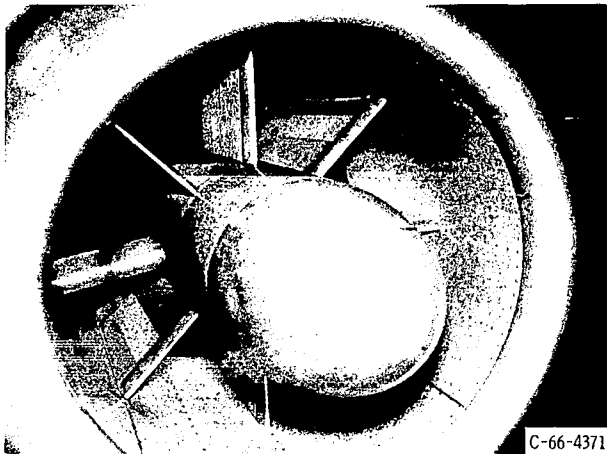
SUPPRESSOR CONSIDERATION AND DESIGN

In designing the experimental inlet noise suppressor, the fundamental considerations were the noise reduction properties and the ease of construction. Some of the other factors that must be considered in applying suppressors to commercial aircraft are weight, size, aerodynamic losses, and safety (ref. 2).

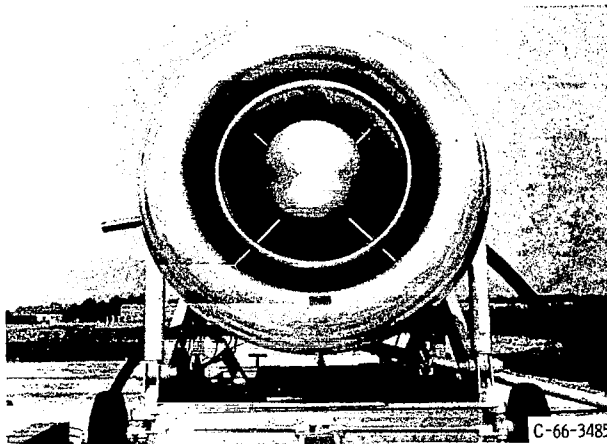
Considerations for the basic design of inlet noise suppressors include both the geometric arrangement of treated surfaces and the type of treatment. Both factors influence the directivity of the propagated sound and the overall sound reduction. The method of treatment chosen for this design was the same as that described in reference 2. The treatment consists of lining the inlet surfaces with 30- to 35-rayl acoustic pressed-metal fiber liner with a 1-inch (2.54-cm) air cavity behind it. Two of the chosen geometric designs included acoustically treated radial-inlet struts, and the third



(a) Basic noise suppressor with four struts.



(b) Noise suppressor with seven struts.



(c) Noise suppressor with four struts and splitter ring.

Figure 1. - Noise suppressors.

included treated radial struts and a circumferential splitter ring. These three configurations of the basic suppressor design are shown in figures 1(a) to (c). For ease of construction, all cowling surfaces were made cylindrical. The basic suppressor is shown in figure 1(a). The suppressors shown in figures 1(b) and (c) were constructed by adding hardware to the suppressor shown in figure 1(a). To prevent inlet flow restrictions, the cross-sectional flow area of the basic suppressor was made equal to the engine inlet area. The open cross-sectional areas of the other suppressors were reduced less than 10 percent by the addition of the struts and splitter. The dimensions of these configurations are given in figure 2. The acoustically treated surfaces include the inside of the cowling,

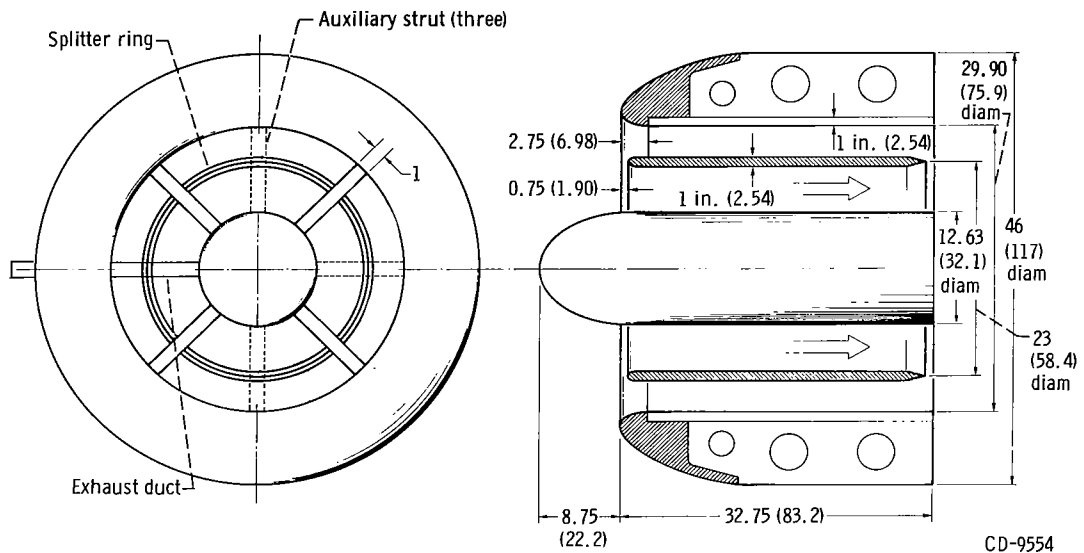


Figure 2. - Inlet-suppressor cowling dimensions. (All dimensions are in inches (cm).)

the outside of the centerbody, the struts, the splitter ring, and the duct cover, which is used to exhaust the smoke from the powder-charge starter cartridge used on the J-65 engine. The struts and splitter ring are covered on both sides by the 30- to 35-rayl material and have a 1-inch (2.54-cm) internal air gap. The inside of the cowling has a 1-inch (2.54-cm) air space and 16 solid longerons for support. The total treated surface area for the suppressors shown in figures 1(a) to (c) are 36, 47, and 66 square feet (3.3, 4.3, and 6.1 m²), respectively.

A hard inlet cowling was constructed to provide a reference for measuring noise attenuation (fig. 3). This cowling has the same length and cross-sectional area as the basic noise suppressor.

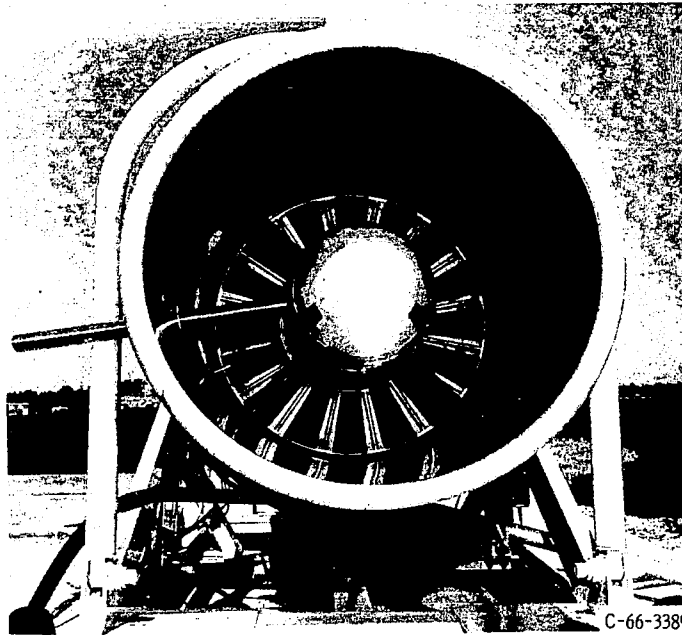


Figure 3. - Modified J-65 engine with hard cowling inlet.

NOISE TEST FACILITIES

Noise Source

To test the attenuation properties of the inlet noise suppressor, a jet-engine noise source having the properties of a turbofan was desired. A turbofan generates discrete blade-passage frequency noise as well as broadband compressor noise. The noise source was a J-65 turbojet engine that had to be modified to produce the discrete blade-passage frequency noise. This engine was easily modified to obtain blade-passage frequency noise, which is generated by stator-rotor interaction on the airflow. Past research has shown that increased noise is generated by (1) increasing the magnitude of the wakes behind stators, and (2) making the number of rotor blades and the number of stator blades similar (ref. 3). Figure 3 shows the modified engine used to create the discrete blade-passage frequency noise. Sixteen flat steel plates were spaced symmetrically around the inlet to block every third inlet guide-vane opening, which increases the wake strength behind the remaining opening and also effectively lowers the number of inlet-guide vanes from 48 to 32, a number close to that of the rotor blades (37). Consequently, by this modification, increased noise at the blade passage-frequency was achieved.

A test was run on the engine to determine the speed that gave the least jet-noise interference with the compressor noise measurements. The jet noise is the low-frequency (mostly under 1 kHz) noise emitted from the rear of the engine and is dominant at high engine speed. The compressor noise is primarily above 1 kilohertz and is propagated out the inlet toward the front engine quadrants of the turbojet. Figure 4 shows

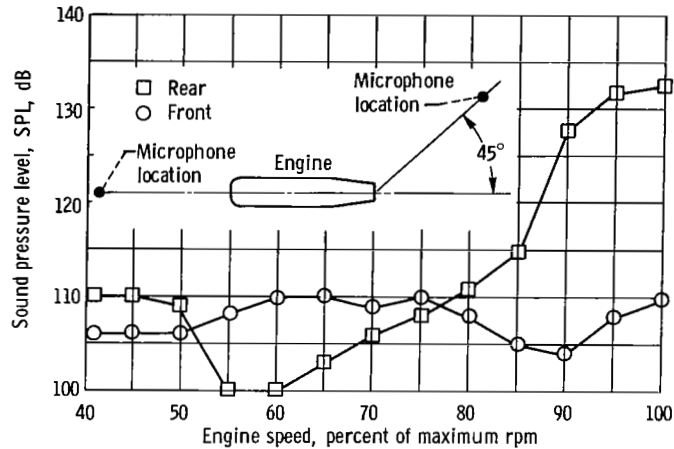


Figure 4. - Noise 100 feet (30.5 m) from J-65 engine.

the overall readings of sound pressure level (SPL) taken at 100 feet (30.5 m) in front of the engine to estimate compressor noise and at 100 feet (30.5 m) 45° from the rear of the engine to estimate jet noise as a function of speed. A rotational speed of 58 percent of maximum rpm (8300) provided a maximum ratio of front to rear engine noise. Consequently, this speed became the operating point for all suppressor noise-reduction measurements. The blade-passage frequency for this speed is 3 kilohertz.

Test Site and Instrumentation

The noise measurements were made in an outdoor environment in a horizontal plane in front of the engine. The engine and suppressor were mounted on a test stand with the center axis 3.5 feet (1.07 m) above ground. One microphone on a stand 3.5 feet (1.07 m) high was moved in 10° increments around a frontal quadrant of the engine from 0° directly in front to 90° at the side. Five spectral data records were taken at each of these 10 angles at several far-field radii. The terrain was a flat concrete apron with no building reflections affecting the data by more than 1/2 decibel.

Noise data were acquired and analyzed on commercially available equipment. The



output of the condenser microphone with a cathode follower and 300 feet (91.5 m) of cable had a variation of less than ± 2 decibels in normal-incidence pressure response from 100 hertz to 10 kilohertz. A one-third octave analyzer obtained spectral plots. Sound pressure level (SPL) averages, perceived noise decibels (PNdB), and sound powers (PWL) were obtained by digitizing the spectral frequency data from 1 to 6.3 kilohertz and processing it in a digital computer.

Measurements were made to determine inlet aerodynamic performance, including inlet static pressures, total pressures, barometric pressures, and air temperature. These measurements were taken in a separate series of tests from those of the noise data.

The total pressures at the cowling exits were measured by four 14-tube survey rakes. The rakes were oriented radially 1.75 inches (4.45 cm) behind the engine-cowling interface. The suppressor designs did not change the flow passages at the location of the rakes; therefore, the flow area at that station remained the same regardless of the type of cowling installed.

The rakes are shown in the installation diagram of figure 5. They consisted of three clusters of four tubes to measure the flow distortions from the splitter ring, the outer surface boundary layer, and the centerbody boundary layer. One tube was located in the center of the flow passage on both sides of the splitter rings. The circumferential positions of the rakes are shown in figure 6. These rakes were installed in only one side of the engine, two placed on the vertical centerline and two located 22.5° off the horizontal centerline. The location of the static-pressure taps is also shown in figure 6. Three taps were installed on the opposite side of the engine, and one was installed

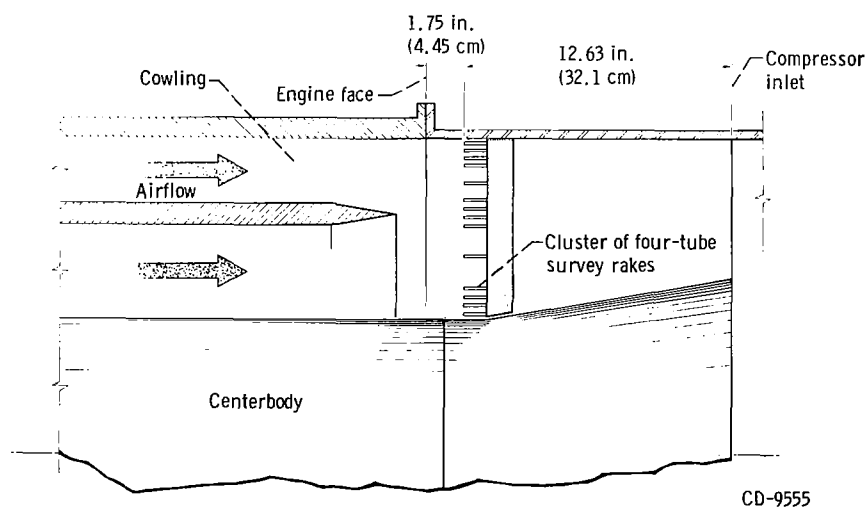


Figure 5. - Location of survey rakes in engine.

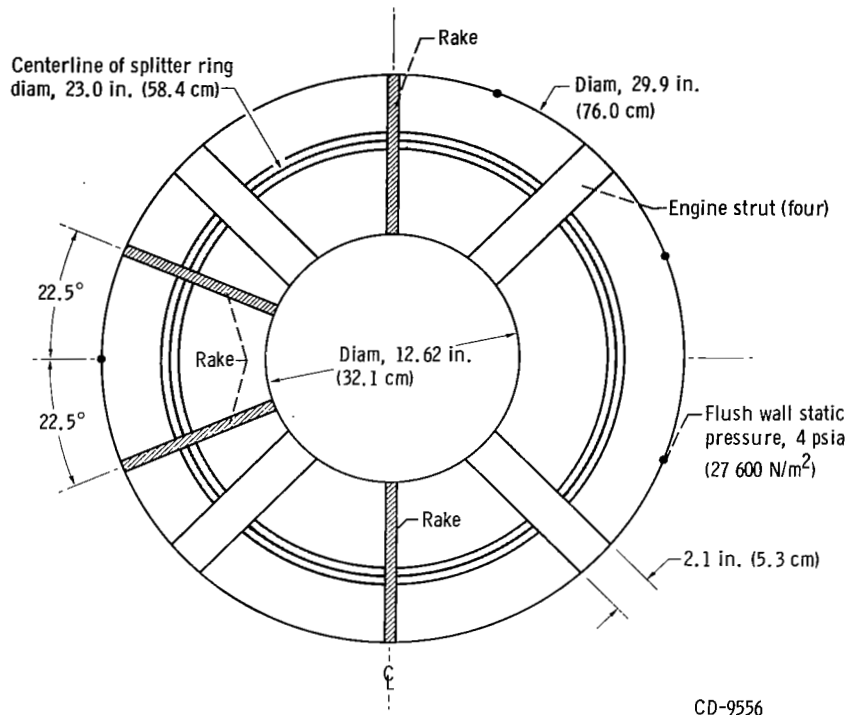


Figure 6. - Location of pressure survey rakes (aft face of cowling looking forward).

between two of the rakes. All four taps were manifolded and read out on an absolute pressure gage with a range of 0 to 15 psia (0 to 103 000 N/m² abs).

The transducers and the recorder were calibrated directly for pressure before and after each run to maintain an error of less than ±0.01 psig (68.9 N/m² gage).

ANALYSIS OF SUPPRESSOR NOISE DATA

Sound Pressure Level

The primary noise data were analog sound-pressure-level spectrographs of the engine noise with the hard cowling and the three suppressor-cowling configurations. Values from five redundant graphs, averaged to give the spectral values of sound pressure level as a function of azimuth position, are presented in table I. The values represent measurements taken at a 100-foot (30.5-m) radius.

A plot of sound pressure level for the hard cowling and noise suppressors is presented in figure 7. The curves display the overall noise values given in table I and characterize engine noise levels measured 100 feet (30.5 m) from the inlet. The



TABLE I. - AVERAGE ONE-THIRD-OCTAVE

SOUND-PRESSURE-LEVEL DATA

[Radius of duct, 100 ft (30.5 m); rotational speed, 58 percent of maximum rpm.]

Frequency, kHz	Angle of measurement, deg									
	0	10	20	30	40	50	60	70	80	90
Hard cowling inlet										
1.0	95	95	93	92	91	88	88	83	81	79
1.2	96	96	95	94	92	89	88	84	83	79
1.6	97	96	95	94	94	92	91	86	84	81
2.0	100	99	97	95	96	94	94	88	86	83
2.5	105	105	106	105	104	100	98	94	92	89
3.1	112	110	114	112	111	107	104	102	99	96
4.0	105	104	105	104	103	98	97	93	89	86
5.0	105	105	104	104	102	97	97	93	89	86
6.3	106	108	107	106	106	102	101	98	93	90
Overall average	116	117	118	117	115	110	108	105	102	101
Four-strut configuration										
1.0	92	90	89	87	85	82	79	77	75	74
1.2	92	92	91	88	85	82	79	77	76	74
1.6	93	92	91	90	85	82	79	76	76	74
2.0	93	93	91	89	88	83	80	77	75	74
2.5	102	103	102	95	95	88	86	84	77	76
3.1	107	108	111	101	103	96	94	93	85	85
4.0	102	101	100	96	94	88	85	81	79	78
5.0	104	102	100	95	93	87	83	80	77	77
6.3	105	103	103	99	96	93	88	83	81	79
Overall average	113	112	116	108	106	101	99	98	94	94
Seven-strut configuration										
1.0	91	90	89	87	84	82	80	76	74	74
1.2	92	91	90	87	84	82	79	77	76	75
1.6	93	93	91	89	85	81	79	76	75	75
2.0	93	92	91	88	86	83	80	75	75	75
2.5	101	102	101	96	93	87	84	81	78	78
3.1	107	109	109	104	101	95	91	85	82	80
4.0	103	101	100	96	92	88	83	77	77	76
5.0	104	101	100	95	92	87	82	78	76	76
6.3	107	104	104	100	96	92	86	81	80	80
Overall average	113	113	113	108	105	99	95	95	93	93
Four-strut-plus-splitter-ring configuration										
1.0	90	88	87	85	83	80	79	77	75	73
1.2	91	90	88	86	83	81	79	78	75	74
1.6	90	89	87	85	83	80	79	77	75	73
2.0	89	88	88	85	83	80	80	76	74	73
2.5	95	94	97	94	92	89	85	83	79	77
3.1	99	101	106	101	101	97	93	90	86	82
4.0	99	98	95	93	88	84	83	80	77	76
5.0	104	99	96	92	88	84	81	78	75	73
6.3	105	101	99	97	93	87	85	81	79	77
Overall average	109	108	109	106	104	100	97	97	93	93

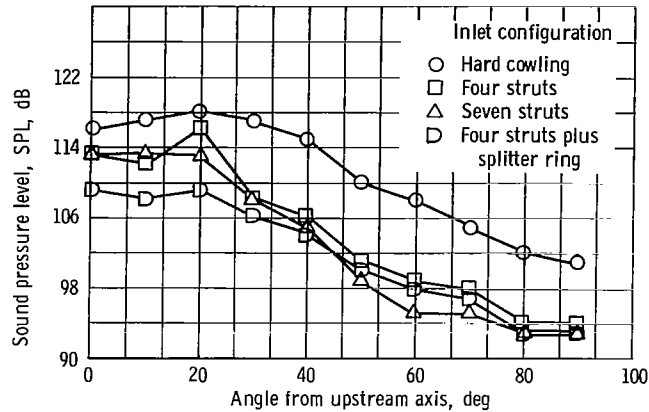


Figure 7. - Noise with various cowling treatments.

maximum values of sound pressure level seem to occur at an angle approximately 20° from the upstream axis of the engine. The sound-pressure-level noise reductions range from 2 to 13 decibels, with the four-struts-plus-splitter configuration clearly achieving the greatest noise reduction (7.5 dB) toward the front of the engine. At the larger, or sideline, angles, the seven-strut configuration has slightly better noise reduction properties in comparison with the other configurations. It is difficult to judge by the curves in figure 7 which configuration is the best noise suppressor for an over-flying aircraft.

Sound Power Reduction

Discussion of experiment. - One method of analyzing the noise data given in table I is to calculate the total sound-power-level (PWL) output coming from the inlet. With this method, the directionality properties of the noise are lost, but the sound-power-level calculations reduce all the sound-pressure-level data in figure 7 to four numbers representing figures of merit for the engine inlet cowlings. These numbers are easier to use in describing the noise-reduction capability of a suppressor and in correlating this capability with the geometric and physical characteristics of each suppressor.

Sound-power-level calculations were performed on the sound-pressure-level data of table I. The sound-pressure-level values at each azimuth angle were converted to intensities and multiplied by a weighted surface area for each angular position. The total surface area considered was a quadrasphere (radius of 100 ft or 30.5 m) in front of the engine and above ground. The end results are sound power values obtained by the integration of the propagated sound intensity over the surface through which it travels. These values are given in table II and show the total sound power and the sound power in each one-third-octave frequency band for each cowling configuration. The attenuation

TABLE II. - ONE-THIRD-OCTAVE SOUND-POWER-LEVELS
FOR COWLING CONFIGURATIONS

Frequency, kHz	Sound power level, PWL, 10^{-13} W			
	Inlet configuration			
	Hard cowling	Four struts	Seven struts	Four struts plus splitter ring
1.00	133.4	128.1	127.6	126.3
1.25	134.6	128.9	128.2	127.0
1.60	136.0	129.4	129.1	126.5
2.00	137.8	130.0	129.3	126.3
2.50	145.5	138.5	137.8	134.5
3.15	152.6	146.1	145.3	143.0
4.00	144.4	137.3	137.0	133.4
5.00	143.8	137.2	136.7	134.1
6.30	147.0	140.0	140.8	137.0
Overall average	157.0	151.0	149.3	146.7

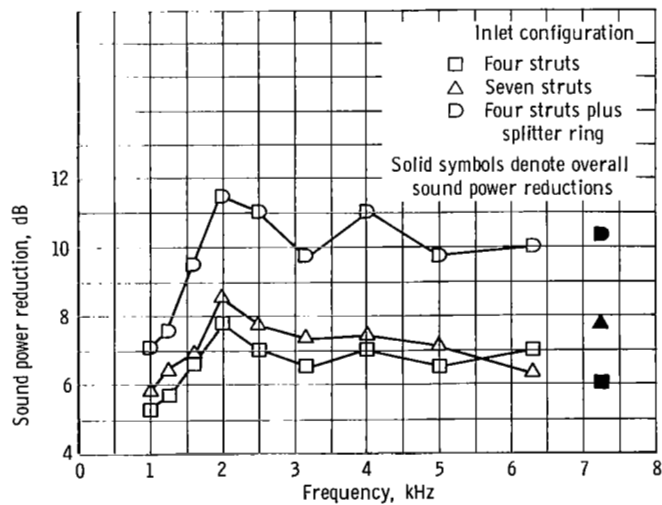


Figure 8. - Spectrum of noise reduction.

of noise by each of the suppressor cowlings in comparison with that of the hard cowling is plotted in figure 8. This figure shows overall sound power reductions of 10.2, 7.6, and 6.0 decibels, respectively, for the four-strut-plus-splitter, the seven-strut, and the four-strut configurations. These sound power reductions are equal to space averaged sound-pressure-level reductions.

Sound-power-level reductions for the three suppressor cowlings occurred over a broad frequency band. Figure 8 shows that their attenuation did not vary by more than 1 decibel from 2.5 to 6.3 kilohertz. The error of the sound-power-level data is roughly ± 0.5 decibel. Hence, the only significant deviations from a flat response are at the 2.0-kilohertz point, where a possible absorption-resonance effect is observed, and at the frequencies below 1.25 kilohertz, when the attenuation properties of the suppressor start to decline significantly.

Previous attempts have been made to correlate overall sound-power-level reduction with physical and geometric properties of inlet noise suppressors (ref. 2). In the following section, an analytical equation for sound-power-level attenuation is derived and is shown to correlate with the experimental sound-power-level reductions obtained herein.

Development of analytical model. - The properties of waves transmitted through a suppressor have not been obtained for the complex geometry, complex waveform, and low wall impedance present in this experiment. However, reference 4 gives an equation for the propagation of plane waves transmitted axially through a cylindrical duct of large wall impedance. In spite of the differences between the conditions of the present experiment and those considered in the equation of reference 4, it is of interest to compare the predicted results of the equation with the experimental data.

The sound pressure response within a cylinder is given in reference 4 as

$$P_s \approx A_0 \left(1 + \frac{i\omega r^2}{2Rc\xi} \right) \exp \left[-\frac{\kappa x}{R} - i \left(\frac{\omega}{c} + \frac{\sigma}{R} \right) x - i\omega t \right] \quad (1)$$

The damping term $\exp(-\kappa x/R)$ in equation (1) can be converted into an equation linking sound-power-level attenuation to properties of the acoustic inlet liner. All symbols are defined in appendix A.

If only the damping term in equation (1) is considered, then

$$P_s \approx B \exp \left(-\frac{\kappa x}{R} \right) \quad (2)$$

and the sound-pressure-level decay is exponential with the axial distance x and with the acoustic conductance ratio κ . Differentiation of the defining equation for sound

pressure level with respect to x yields

$$\frac{d}{dx} (\text{SPL}) = 20 \frac{d \left(\log \frac{P_s}{P_{\text{ref}}} \right)}{dx} = -8.68 \frac{\kappa}{R} \quad (3)$$

Equation (3) gives the ratio of sound-pressure-level attenuation in decibels to the change in axial distance x along the suppressor. A more useful attenuation criterion than the overall suppressor length L and radius R is the inlet cross-sectional area A and its treated wall surface area $2\pi RL = S$. These dimensions can be written as a ratio in equation (3) if the numerator and denominator are multiplied by $2\pi R$. Then, integration with respect to length yields

$$\Delta(\text{SPL}) = -4.34 \kappa \frac{S}{A} \quad (4)$$

Since a difference in sound pressure level is equivalent to the same difference in sound power level when both are given in decibels, then

$$\Delta(\text{PWL}) = (-4.34 \kappa) \frac{S}{A} \quad (5)$$

Equation (5) states that sound power reduction in an acoustically treated cylinder with axially propagating waves is directly proportional to the acoustic conductance ratio κ and to the area ratio S/A .

The noise results obtained from the inlet suppressor configurations were used to test equation (5). A graph of the noise-power-level reduction as a function of the area ratio for the three inlet suppressors is presented in figure 9. A straight line can be drawn through the data points and the origin to within the data error of ± 0.5 decibel. Noting that the suppressors were not simply acoustically treated cylinders, one must conclude from figure 9 that, even where the treated area is distributed over a centerbody, the struts, the splitter assemblies, and a cylinder, rather than on a simple cylinder, the change in sound power level is still directly proportional to the area ratio S/A .

The direct relation of κ to noise power attenuation in equation (5) was not experimentally shown by the suppressor data since all suppressors had the same type of acoustic treatment and, consequently, the same value of κ . This value of κ can be calculated from equation (5) and the suppressor noise data. From figure 11, the value of κ is 0.13. Since the correctness of this value for κ is determined by the applica-

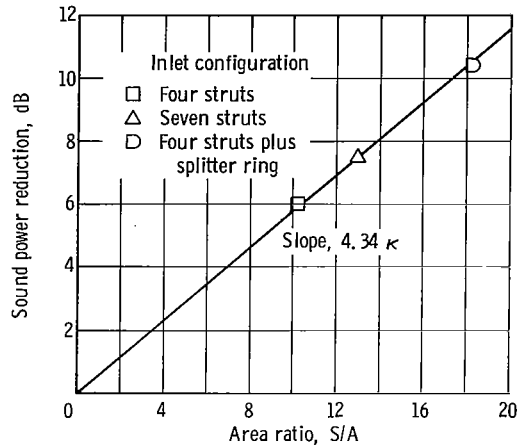


Figure 9. - Correlation of noise reduction with acoustically treated area.

bility of equation (5) in predicting the noise attenuations, an independent determination of κ from another source is desired for a comparison.

Generally, the conductance ratio κ can be expected to be a function of frequency; therefore, a value for κ was calculated at each one-third-octave frequency from the data in figure 8 just as the overall value was calculated from figure 9. The results for all three suppressors are plotted as the lower curve in figure 10. The value of κ is the same for each suppressor, since the same type of acoustic treatment was used. The frequency response is relatively flat because κ is derived from the sound-power-level

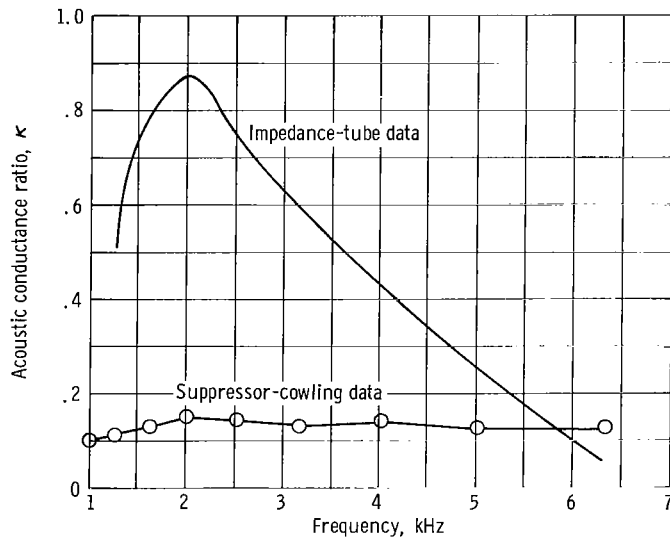


Figure 10. - Acoustic conductance characteristics of suppressor liner of 30- to 35-rayl pressed-metal fiber with 1-inch (2.54-cm) air backing.



spectrums of figure 8, which are also relatively flat. All spectral values of κ from 1 to 6.3 kilohertz are within 20 percent of the overall value of 0.13 given in equation (6).

Impedance-tube measurements (ref. 2) were used to obtain a value of acoustic conductance to compare with the value predicted by the suppressor noise data presented herein. The acoustic resistance and reactance are given in reference 2 for a 30- to 35-rayl liner material with a 1-inch (2.54-cm) air backing. The conductance κ can be computed from the resistance θ and the reactance χ by

$$\kappa = \frac{\theta}{\theta^2 + \chi^2} \quad (6)$$

This equation is plotted as the upper curve in figure 10. These values for κ differ greatly from those calculated for the suppressor cowlings with equation (5). The first of four possible reasons for this difference is that the impedance-tube measurements were taken with noise intensities of 120-decibel SPL instead of with the 150- to 160-decibel SPL levels that are incurred in the suppressor inlets. These high intensities cause nonlinear flow characteristics in the liner material, which increase its acoustic resistance. From equation (6) it can be seen that an increase in acoustic resistance would both lower the value of κ , and, since resistance changes little with frequency, cause the curve of κ against frequency to become flatter. These two trends are required to make the upper curve of figure 10 approach the lower curve.

A second reason for the difference between the curves concerns the airflow across the acoustic liner material. Impedance-tube measurements were obtained with no airflow, whereas the inlet suppressors had inlet flow velocities up to Mach 0.55 across their surfaces. The airflow across the liner surface also increases the acoustic resistance, which modifies the value of κ (ref. 5).

The third reason the curves differed is that the air cavity behind the suppressor lining was not compartmentalized. In the absence of compartmentalization, sound waves can propagate in the backing cavity of the liner, which could result in a decrease in attenuation characteristics of the liner. Experiments have shown that the attenuation properties of a liner are approximately doubled with compartmentalization (ref. 6).

The fourth reason for the deviation in the curves of figure 12 is that the assumptions going into equation (5) might be too general to apply to the suppressor. Thus, while the impedance-tube data give a qualitative indication that equation (5) might be an accurate model for predicting suppressor noise reduction, it still cannot be proved exact at this time because of a lack of data.

The third reason suggests several ideas for improvements to the acoustic liner. The use of a compartmentalized liner would increase the value of κ (ref. 5). In addition, impedance-tube data on 25-rayl liner material obtained from reference 2 showed

that this material would have a higher κ and, consequently, a better attenuation property according to equation (5).

Another important interpretation of equation (5) concerns full-scale suppressor tests of various acoustical treatments. This equation implies that geometric configuration is not a major factor in total sound power attenuations as studied herein. Neither the number of struts nor the addition of a splitter ring significantly varied the shape of the sound-power-level response in figure 8. The purpose of the splitter, other than to increase the overall treated surface area, was to provide a treated-surface separation distance of about $1/2$ wavelength. From figure 4, the separation distance is 6 inches (15.2 cm), which corresponds to a frequency of about 2 kilohertz. It was hoped that the $1/2$ -wavelength separation would increase the attenuation at 2 kilohertz. A slight increase in attenuation was achieved at 2 kilohertz for the splitter configuration in figure 8, but generally the varying geometry had little effect. Thus, a simple cylindrical inlet suppressor can be designed and tested. The sound power attenuation for any other configuration with a larger or smaller treated surface area can then be extrapolated from the results for the simple inlet suppressor.

Human Response

The noise perceived by a ground observer of overflying engines with and without inlet suppressors was calculated and compared. The annoyance response of the observer was taken into account by the use of the perceived-noise-frequency-weighting factors. The resulting PNdB values take into account both the directionality and frequency spectrum effects on an observer of the various suppressors. Therefore, another means is provided for rating suppressor-noise-reduction ability.

The model for PNdB calculations assumes a low forward-speed flyover at an 800-foot (244-m) altitude with a 0° angle of attack on the engine. The effects of a high-speed flyover (Doppler frequency shift, etc.) were not considered. The sound-pressure-level data given in table I are presumed to apply to the vertical plane in front of the engine as well as to the horizontal plane. Ground reflection errors that would distort the vertical pattern at 800 feet (244 m) of altitude are negligible. Thus, the SPL data can be extrapolated to ground level along the projected flight path by assuming a 6-decibel attenuation for every doubling of the distance from the source. These ground level SPL values are then converted to PNdB readings by procedures outlined in reference 6.

The PNdB flyover noise for the hard cowl and each suppressor is tabulated in table III and shown in figure 11. Maximum PNdB attenuations of 6.3, 7.5, and 10.5 PNdB were obtained for the four-strut, seven-strut, and four-strut-plus-splitter

TABLE III. - PERCEIVED-NOISE-DECIBEL VALUES FOR CALCULATED
800-FOOT (244-m) FLYOVER

	Inlet configuration			
	Hard cowling	Four struts	Seven struts	Four struts plus splitter ring
Ground distance from approaching engine, ft (m):				
0 (0)	94.6	85.2	82.8	82.8
139 (42.4)	97.5	85.7	83.6	85.6
299 (91.3)	100.4	90.8	85.6	89.2
469 (143)	102.3	91.8	89.8	90.9
661 (202)	101.9	93.4	93.0	93.3
952 (291)	106.1	98.6	97.0	95.6
1384 (422)	104.9	95.5	97.7	95.0
2200 (671)	102.8	99.8	98.6	95.2
4536 (1384)	95.1	92.6	93.3	88.3
Maximum perceived noise decibels	106.1	99.8	98.6	95.6
Maximum perceived noise-decibel-attenuation, Δ PNdB	-----	6.3	7.5	10.5

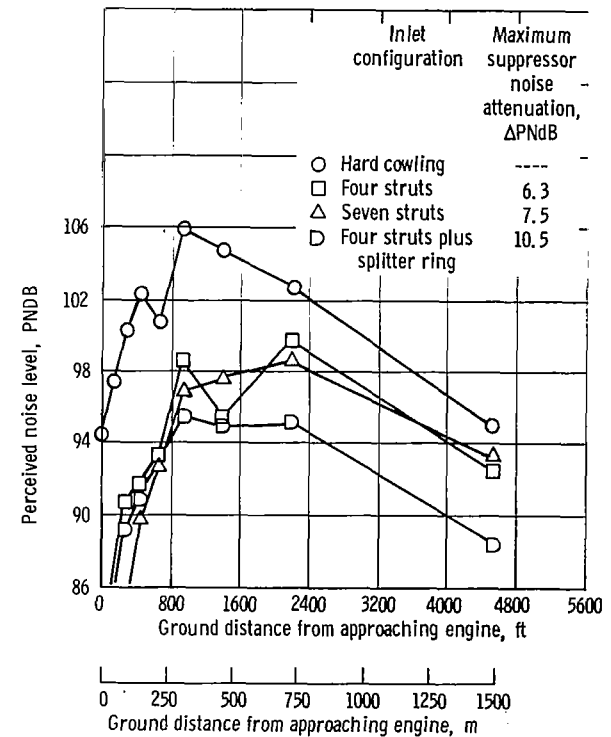


Figure 11. - Perceived-noise-decibel level for simulated flyover at 800 feet (244 m).

configurations, respectively. The reason these PNdB attenuations are so similar to the sound-power-level attenuations is that the inlet geometry has little effect on redirecting the noise (fig. 7). All three suppressors are effective at reducing the noise directly under the engine. As a result, maximum PNdB values occur when the observer is well ahead of the approaching engine - at 1000 feet (305 m) in front of the engine for both the hard cowl and the four-strut-plus-splitter configurations, and at 2200 feet (671 m) for both the four-strut and the seven-strut configurations. These distances are equivalent to the 20° to 40° angles from the upstream engine axis.

Aerodynamic Measurement Discussion

The internal-flow losses of the noise-suppressor cowling were obtained by calculation of a mass-flow weighted inlet pressure drop from the total-pressure survey, the static-pressure survey, the barometric pressure, and the air temperature. These calculations are given in appendix B. In final form, the inlet pressure drops are divided by the ambient air pressure to form a pressure-loss coefficient that is plotted against a corrected engine speed (see appendix B) in figure 12. The results of both the four-strut and the four-strut-plus-splitter ring configurations are also shown.

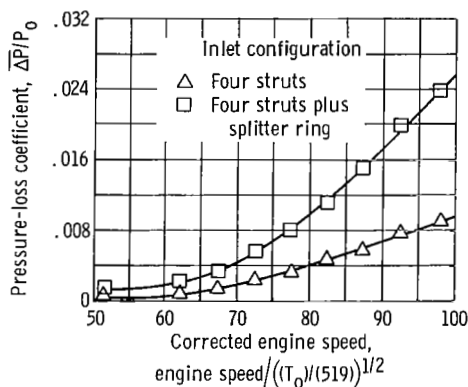


Figure 12. - Internal flow losses of noise-suppressor cowlings.

The four-strut configuration was used as a basis of comparison because the flow restriction was small, and the inlet lip was fairly well shaped. At rated (100 percent) engine speed, the four-strut suppressor had a pressure-loss coefficient of 0.010, and the addition of the splitter ring increased this to 0.026.

The effect of the splitter ring on the flow distortion is shown by the pressure pro-



files for the annulus at the cowling exits. These profiles are plotted in figure 13. The data from this survey were taken at about $97\frac{1}{2}$ percent corrected engine speed for both suppressor cowls. The depth of the boundary-layer distortions at both inner and outer surfaces was about the same on the two suppressor cowls. Because of the higher flow velocities caused by the restriction from the splitter, the magnitude of the distortion was larger at both surfaces.

The major contributing factor to the difference in loss coefficients of the curves in figure 13 is the boundary-layer buildup on the splitter surfaces. Nearly half of the measured flow loss was in the wake of the splitter rings.

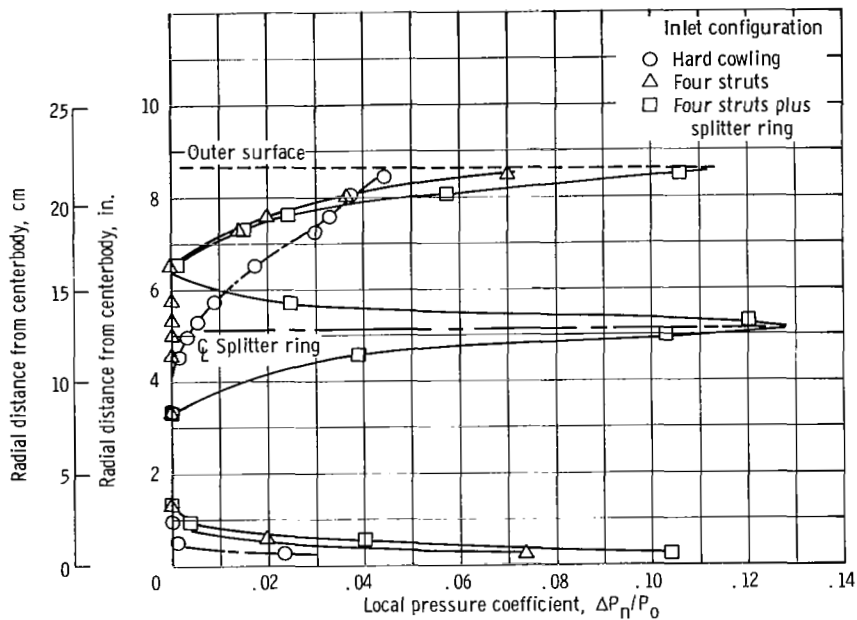


Figure 13. - Pressure profiles at cowl exits at 95 percent maximum engine speed.

It is important to point out that there seems to be no evidence of boundary-layer thickening at the cowl exits by flow through the porous surface and flow from the cavity. Because the outer surface liner and cavity were constructed with longitudinal struts, as opposed to ring bulkheads, there were no barriers to longitudinal flow in the cavity when a pressure gradient existed in the cowling. If such a gradient were to occur, air would circulate behind the porous material and come out the inlet end, and a large flow distortion would result. A comparison of the pressure profiles obtained for the hard, smooth reference cowl with those of the lined cowls should have shown whether or not air was blowing through the porous surface from the back cavity. However, the refer-

ence cowl was constructed with such a poor lip that its flow losses were about 50 percent higher than those of the four-strut suppressor cowl, and the comparison was obscured. The pressure-loss-coefficient profile for the reference cowl is represented by the dash-dot curve in figure 13. When the reference profile is compared with that of the suppressor cowls, it is evident that the magnitude of the reference cowl loss is somewhat smaller, but this loss-coefficient profile penetrated much deeper into the flow passage.

The test facility contained no thrust measuring apparatus; therefore, the flow loss coefficients could not be directly correlated with the performance loss. However, the effect of duct inlet losses on performance as an inverse relation with engine pressure ratio can be shown. With the use of an engine pressure ratio of 2.2 as typical of the turbojet engine employed in this experiment, a thrust loss factor was calculated as $1.8(\overline{\Delta P}/P_0)$ for the present tests. However, a turbofan engine may have a pressure ratio of only 1.3. A thrust loss factor of $3(\overline{\Delta P}/P_0)$ may then be obtained. Therefore, if the splitter-ring-type noise suppressor were installed on either engine, a thrust loss of 4.7 percent could exist for the turbojet and a loss of 7.8 percent could exist for the turbofan.

CONCLUSIONS

Significant far-field noise attenuations were obtained with broadband-resonator-type inlet noise suppressors on a full-scale engine. Noise-reduction characteristics obtained by sound power and simulated flyover perceived-noise-decibel calculations showed a maximum reduction in sound power of 10.2 decibels and a maximum reduction in flyover noise of 10.5 perceived noise decibels. Both these values were obtained with the four-strut-plus-splitter ring configuration.

Experimental total sound power reductions correlated with the ratios of acoustically treated surface area to cross-sectional area of the inlets. These ratios were derived from an analytical calculation for sound power attenuation in a cylindrical duct, but they apply equally well to the inlet-suppressor geometries that were tested. The analytical equation also related sound power attenuation to the acoustical conductance of the treatment. An attempt was made to correlate the acoustic conductance from the suppressor experimental results with limited impedance-tube measurements obtained by other investigators. The results show a lack of agreement which is probably a result of the systematic differences in conditions between the two tests. The values of the acoustic conductance calculated from the suppressor data were nearly constant functions of frequency in the range of 1.6 to 6.3 kilohertz. Thus, the attenuations were constant over this range.

Varying the inlet geometries had no measurable effect on the overall noise reduction and had only a small effect on the directionality of sound propagation. Struts reduced

sideline noise, whereas cylindrical surfaces reduced front noise. Maximum perceived-noise-decibel values for an engine-flyover calculation occurred off axis at angles from 20° to 40° with respect to the inlet.

Engine inlet pressure losses caused by the blockage effects of the suppressor treatments were calculated to be no worse than 2.6 percent at full speed. This loss occurred with the four-strut-plus-splitter-ring configuration.

These results show that jet-engine inlets can be acoustically treated to reduce noise significantly. The present analysis indicates that compartmentalization of the air space behind the liner and the use of a lower resistance metal-fiber liner could significantly increase the noise reductions obtained in the present study.

Lewis Research Center,
National Aeronautics and Space Administration,
Cleveland, Ohio, February 21, 1968,
126-15-01-21-22.

APPENDIX A

SYMBOLS

A	cross-sectional area of engine inlet cowling	$\overline{\Delta P}$	overall weighted pressure drop for given inlet configuration
A_n	weighted cross-sectional area for n^{th} total-pressure sample in inlet aerodynamic measurements ($n = 1$ to 14)	R	radius of duct
A_o	peak pressure amplitude	r	radial position in duct
B	peak pressure amplitude	S	treated surface area in suppressor inlet
c	speed of sound	T_o	outside air temperature
L	length of inlet-suppressor cowling	t	time
P	inlet aerodynamic pressure drop	x	axial distance along inlet-suppressor cowling progressing toward front
P_n	aerodynamic total pressure drop averaged for n^{th} radial position	ζ	complex acoustic admittance
P_o	barometric pressure	θ	acoustic resistance
P_{ref}	reference sound pressure, -0.0002 microbars	κ	acoustic conductance ratio
P_s	inlet sound pressure	σ	acoustic susceptance
P_1	absolute wall static pressure at inlet survey station	χ	acoustic reactance
		ω	angular frequency



APPENDIX B

AERODYNAMIC CALCULATIONS

The aerodynamic data used to calculate inlet flow losses include a total-pressure survey, static-pressure taps, barometric ambient air pressure, and air temperature.

The total-pressure survey made with four 14-tube rakes was the fundamental data used in obtaining the inlet pressure drop. The individual pressure readings from each tube were weighted with the corresponding flow areas and local velocities. The weighted values were then totaled into a single value of pressure drop for one survey reading. The method of calculation is as follows: The readings from corresponding tubes in each of the four rakes were averaged arithmetically. These averages along with the corresponding local areas and the static pressures were inserted into the following equation to give the total engine pressure drop:

$$\overline{\Delta P} = \frac{\sum_{n=1}^{14} P_n A_n (P_o - P_n - P_1)^{1/2}}{\sum_{n=1}^{14} A_n (P_o - P_n - P_1)^{1/2}} \quad (B1)$$

Then, dividing by the outside ambient pressure P_o (in psia or N/m^2 abs) normalized the calculated weighted pressure drop for atmospheric-pressure differences. These nondimensional coefficients were plotted against the engine speeds corrected for the outside air temperature and normalized to a standard temperature of $519^{\circ} R$ ($288^{\circ} K$). A corrected engine speed was used because the test facility contained no airflow measuring apparatus. The replacement of airflow by corrected engine speed should be valid over a wide range of engine inlet pressure and temperature (Reynolds number index of 0.2 to 0.8). Thus, the plots show the pressure-loss coefficient $\overline{\Delta P}/P_o$ as a function of the corrected engine speed, which is

$$\frac{\text{Engine speed}}{\left(\frac{T_o}{519}\right)^{1/2}} \quad (B2)$$

REFERENCES

1. Lowson, M. V.: Reduction of Compressor-Noise Radiation. Paper presented at the 72nd Meeting of the Acoustical Society of America, Los Angeles, Nov. 2, 1966.
2. Marsh, Alan H.; Elias, I.; Hoehne, J.C.; and Frasca, R.L.: A Study of Turbofan Engine Compressor-Noise Suppression Techniques. Rep. No. DAC-33170, Douglas Aircraft Co., June 1966.
3. Tyler, J.M.; and T.G. Sofrin: Axial Flow Compressor Noise Studies. Paper No. 345D, SAE, 1961.
4. Morse, Philip M.: Vibration and Sound. Second ed., McGraw-Hill Book Co., Inc., 1948, p. 307.
5. Mechel, F.; Mertens, P.; and Schilz, W.: Research on Sound Propagation in Sound-Absorbent Ducts with Superimposed Air Streams. Final Rep. (AMRL-TDR-62-140, vols. I, II, and III). Physikalisches Inst., Univ. Göttingen, West Germany, Dec. 1962.
6. Phillips, Bert; and Morgan, C. Joe: Mechanical Absorption of Acoustic Oscillations in Simulated Rocket Combustion Chambers. NASA TN D-3792, 1967.
7. Beranek, Leo L.: Noise Reduction. McGraw-Hill Book Co., Inc., 1960.

